SCIENTIFIC RESEARCH

CHARACTERIZATION OF CEREBRAL ANEURYSMS FOR ASSESSING RISK OF RUPTURE BY USING ANEURYSMS FLOW IN DSA

Nguyen Van Hoang*, Vu Dang Luu *, Tran Anh Tuan**, Nguyen Ngoc Trang**, Le Hoang Kien**, Nguyen Quang Anh*, Nguyen Tat Thien**, Nguyen Huu An**, Nguyen Thi Thu Trang**, Tran Cuong **, Tu Duc Ngoc **, Le Hoang Khoe**, Nguyen Thi Hao*, Vu Thi Thanh**, Pham Minh Thong*

SUMMARY

Calculating intra-aneurysm flow uses optical flow with computational fluid dynamics simulation on the numerical analysis. This is a new method to better understand the intravascular flow and aneurysm flow as well as factors related to the inflow vortex and the inflow jet which increase the rupture risk in patients with an aneurysm. It is essential to identify high-risk rupture sites for unruptured aneurysms and elucidate flow characteristics and flow morphology with ruptured aneurysms (RA). Therefore, we implement the study with two aims: 1, determine the hemodynamic factors and the flow rate inside the aneurysm, and 2, compare ruptured and unruptured aneurysms by flow measurement software (Digital Subtraction Angiography (DSA)-AneurysmsFlow on 2-plane DSA machine at Bach Mai hospital.

Subjects and Method: A descriptive cross-sectional study was conducted between July 2021 and July 2022. There were a total of 127 patients with aneurysms who took DSA – AneurysmsFlow and received treatment at Bach Mai hospital.

Results: In 127 patients with 170 aneurysms, there were 139 aneurysms in a different locations which were calculated their flow by the AneurysmsFlow software in DSA at Bach Mai hospital. The flow model was affected mostly by the aneurysm wall, the most frequently seen was in the dome (64.8%), or body (29.1%). Only 15% of the aneurysm showed that the flow affected to aneurysm neck. According to the simple Cebral's classification based on inflow and the formation of the vortex as well as the consistency of the vortex, type I (57.6%) is the most prevalent, next is type IV (19.4%), type II (12.2%), and the last one is the type III (10.8%). Simple consistent aneurysm models, large flow impingement regions, and large inflow jet size were usually seen at unruptured aneurysms. Conversely, rupture aneurysms were likely to have a vortex model, small flow impingement area, and small inflow jet size.

Conclusion: Flow calculation on DSA – Aneurysms Flow helps to understand better the dynamic of flow in the parent artery and aneurysm which help to consider early treatment in high-risk ruptured aneurysm as well are thoroughly understand the dynamic inside the ruptured aneurysm to have a right treatment plan.

Keywords: *intravascular flow, cerebral aneurysm, DSA, Aneurysms.*

** Radiology Department - Hanoi Medical University*

*** Radiology Center - Bach Mai Hospital*

I. BACKGROUND

Cerebral aneurysm (CA) is a fairly common neurological disease, about 0.4-3.6% on gross and 3.7-6.0% on angiography, in which 85% of aneurysms are located in the Willis polygon region. Aneurysm subarachnoid hemorrhage (ASH) accounts for 80-85% of nontraumatic subarachnoid hemorrhage. The mortality rate of ASH can be up to 25%, even if it can be from 32-67% according to S.Claiborne. ASH sequelae can occur in 50% of survivors, so it is important to early monitor and treats CA to avoid rupture complications [1 - 3].

Nowadays, unruptured aneurysms (URA) are increasingly detected in an early stage, the question is which aneurysms should be treated, which one should be monitored, and how to monitor them. Many studies have shown that some factors such as gender, age, race, location, shape, and size of aneurysms are factors related to the risk of aneurysm rupture, in which hemodynamic factors are an important factor but not well understood.

Recently, a new method has been developed based on Digital Subtraction Angiography (DSA). The method combines flow measurement using the optical flow principle (OF) and digital flow dynamic simulation, which allows to observe the blood morphology and dynamic characteristics in patients with intracranial aneurysms. Bonnefous et al [4] a method for the estimation of arterial hemodynamic flow from x-ray video densitometry data is proposed and validated using an in vitro setup.\nMETHODS: The method is based on the acquisition of three-dimensional rotational angiography and digital subtraction angiography sequences. A modest contrast injection rate (between 1 and 4 ml/s successfully validated this OF method for flow rate measurement in vitro experiments, and Pereira et al [5] used DSA to measure the mean aneurysm flow amplitude (MAFA) ratios before and after stenting to demonstrate the effect in reducing intra-aneurysm flow after stent placement and appears as a good prognostic factor for aneurysm thrombosis. Important factors of this technique include low contrast injection rate and application of OF principle to angiography frames with high frame rate [6]. It is essential to identify high-risk rupture sites for URA and elucidate flow characteristics and flow morphology with ruptured aneurysms (RA).

Currently, there is no research on the method of measuring the flow rate in the aneurysm in Vietnam. Therefore, we implement the study with two aims: 1, determine the hemodynamic factors and the flow rate inside the aneurysm, and 2, compare ruptured and unruptured aneurysms by flow measurement software DSA- AneurysmsFlow on 2-plane DSA at Bach Mai hospital.

II. MATERIALS & METHODS

1. Participants

Patients who were diagnosed with CA by radiology modalities such as Magnetic Resonance Imaging (MRI), Multi-slice Computed Tomography (MSCT), DSA - AneurysmsFlow in 2-plane DSA from Phillip at Bach Mai hospital from 07/2020 to 07/2022.

Inclusive criteria:

+ Patients who were diagnosed with ruptured and unruptured aneurysms by DSA – Aneurysms with the right protocol for flow rate.

+ Patients who accepted the intravascular intervention.

Exclusive criteria:

+ Patients who had contrast allergy

+ Patients who had renal failure

2. Study method

Study design: Cross-sectional descriptive study

Study variables:

Aneurysm inflow location

- Aneurysm inflow location is where the flow in the parent vessels enters the first aneurysm, the earliest place is at the aneurysm neck. We divide the neck into the proximal one and the distal one according to the direction of flow. If the position of the neck is near the mother vessel flow, it is the proximal neck. If it is far from the parent vessel flow, it is the distal neck.

Flow impingement region (IR)

- IR: The area is in the aneurysm wall where the incoming stream hit the wall for the first time and changes direction or scatter.

Size of flow impingement region (IS)

- At the flow impingement region, it is assessed as large or small size based on the ratio between the flow impingement region and the location of the aneurysm. Reactions or inflow resistance are considered small if they are less than half of the size of the standard dimension (neck or bottom diameter of the aneurysm).

Size of inflow jet

- The size of the inflow jet is compared to the largest size of the aneurysm and divided into large or small. It is considered small if they are less than half of the size of the standard size (neck diameter of the aneurysm).

Aneurysm flow classification according to JR. Cerebral

Type I: Unchanging direction of inflow jet with a single associated vortex

Type II: Unchanging direction of inflow jet with multiple associated vortices but no change in the number of vortices during the cardiac cycle

Type III: Changing the direction of the inflow jet with the creation of a single vortex

Type IV: Changing the direction of the inflow jet with the creation or destruction of multiple vortices

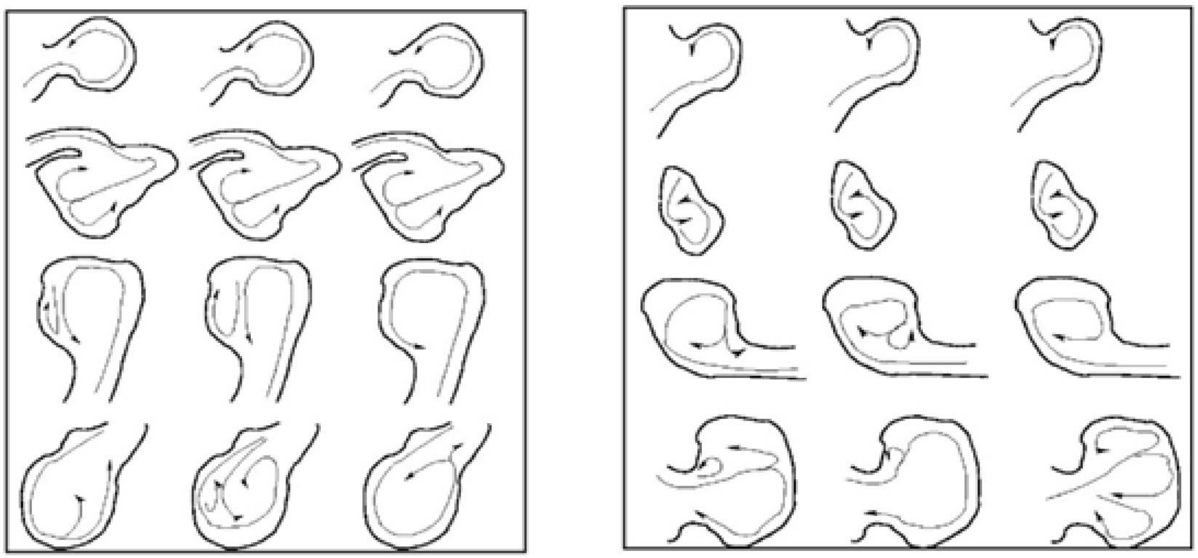

Figure 1. *Schematic drawings of the most prominent flow structures observed in small (left) and large (right) aneurysms with flow types I (top) through IV (bottom). Arrows indicate the direction of flow at 3 instants during the cardiac cycle and illustrate the complexity and stability of the intra-aneurysmal flow patterns for the 4 flow type categories [7].*

Data analysis:

- Data was analyzed by SPSS software version 20.0 (IBM, USA)

III. RESULT

1. Demographic characteristics

The study was implemented in 127 patients with 170 CA. 80 patients were females and 47 patients were male, the female/male rate was 1.7. The mean age was 56.31 years old, the youngest was 27 years old, and the oldest was 84 years old. The proportion of patients with ruptured and unruptured aneurysms was quite similar, with 66 and 61 patients respectively, accounting for 52% and 48%. MSCT is a quick and accurate diagnostic tool in 97% of ruptured aneurysms. DSA detected an additional 19 small aneurysms accounting for 18% of unruptured aneurysms and 11.2% of all aneurysms when previously undetected by MRI and MSCT.

2. CA characteristics

2.1. The amount of CA in patients

Table 1. *The amount of CA in patients*

Aneurysm / Amount/ patient	RA (n=66)		URA (n=61)		p
	n	%	n	%	
1	54	55,7	43	44,3	0,32
2	8	38,1	13	61,9	
≥ 3	4	44,4	5	55,6	
Total	**66**	**52,0**	**61**	**48,0**	

Comments: Most patients had one aneurysm (76.4%), 21 patients (16.5%) had two aneurysms, and 9 patients (7%) had ≥ 3 aneurysms.

2.2. Position and dimension of aneurysm

The internal carotid aneurysm was the most prevalent, accounting for 88 aneurysms (51.8%). The aneurysm in the anterior communicating artery occupied 18.2% and the aneurysm percentage in the posterior communicating artery was 10.6%. The least common aneurysm was in the posterior circulation.

Table 2. *Dimension of CA*

Aneurysm diameter	n	%
< 5mm	113	66,5
5-10 mm	45	26,5
10 – 25 mm	12	7,1
Overall	170	100
Mean diameter	4,83±2,73 (1,10-18,00)	

Comments: Small aneurysms (< 5mm) occupied the majority of the aneurysm in this study, 66.5%. The rate of an aneurysm with a diameter larger than 10mm was 7.1%. The mean diameter was 4,83±2,73.

2.3. Aneurysm neck characteristics

- Wide and narrow-neck aneurysm:

The criteria for a wide aneurysm neck: neck dimension ≥4mm and/ or the height/neck rate <1,5

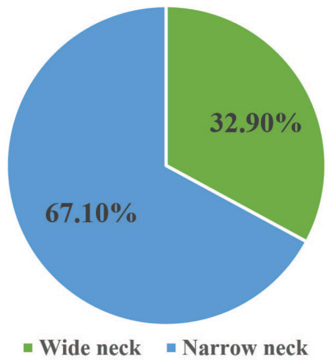

Chart 1. *Distribution of aneurysm diameter*

Comments: Wide-neck aneurysms more than narrow-neck aneurysms, 114 aneurysms (67.1%) and 56 aneurysms (32.9%) respectively.

2.4. Aneurysm flow at different positions

Table 3. *Aneurysm flow at different positions*

	Flow		
	Mean±SD	Min	Max
Parent vessel	3,27±1,18	0,50	6,30
Middle aneurysm	2,86±1,48	0,80	7,80
Neck	3,15±1,69	0,80	8,90
Dome	2,28±1,31 0,60		7,80
Inlet flow	3,14±1,72	0,80	9,30
Output flow	2,89±1,64	0,80	8,20

Comments: The largest flow was seen in the aneurysm neck and the inlet position, 3.15 ml/s and 3.14 ml/s respectively. The lowest flow was seen in the bottom, 2.28 ml/s.

3. Hemodynamic characteristics

3.1. Stream effect on the aneurysm

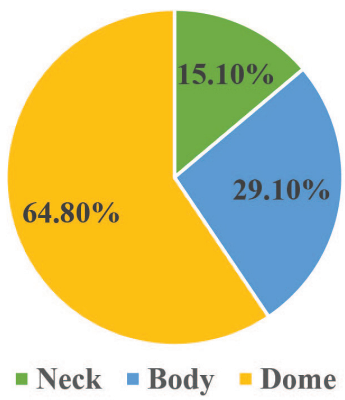

Chart 2. *Stream effect to the aneurysm*

Comments: in 139 aneurysms, the stream was mostly at the bottom (64.8%), then at the body (29.1%). Only 15% of aneurysms are affected by the aneurysm neck.

3.2. Stream to the ruptured aneurysm and unruptured aneurysm.

Table 4. *Stream to the ruptured aneurysm and unruptured aneurysm*

Stream to the aneurysm	RA	URA	Total
Neck (1)	9 (42,9%)	12 (57,1%)	21 (100%)
Body (2)	9 (32,1%)	19 (67,9%)	28 (100%)
Bottom (3)	49 (54,4%)	41 (45,6%)	90 (100%)
Total	67 (48,2%)	72 (51,8%)	139 (100%)
p	0,10		

Comments: There was no significant statistic in the different positions of RA and URA.

3.3. The most common stream to the aneurysm neck

Table 5. *The most common stream to the aneurysm neck*

Neck stream	RA	URA	n
Distal (1)	63	66	129 (92,8%)
Close (2)	4	6	10(8,2%)
n	67		139(100%)

Comments: Most of the stream was to the distal part of the aneurysm neck, 129/139 aneurysms (92.8%).

3.4. Flow classification

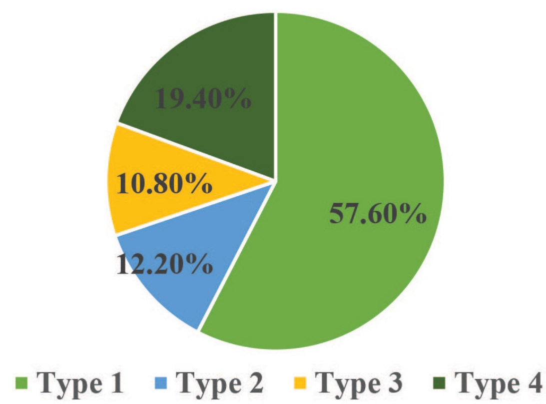

Chart 3. Intraaneurysm flow classification according to the Cerebral classification

Comments: Type 1 occupied the highest percentage (57.6%), next was type IV (19.4%), type II (12.2%), and the last one was

3.5. Stream classification to the RA and URA

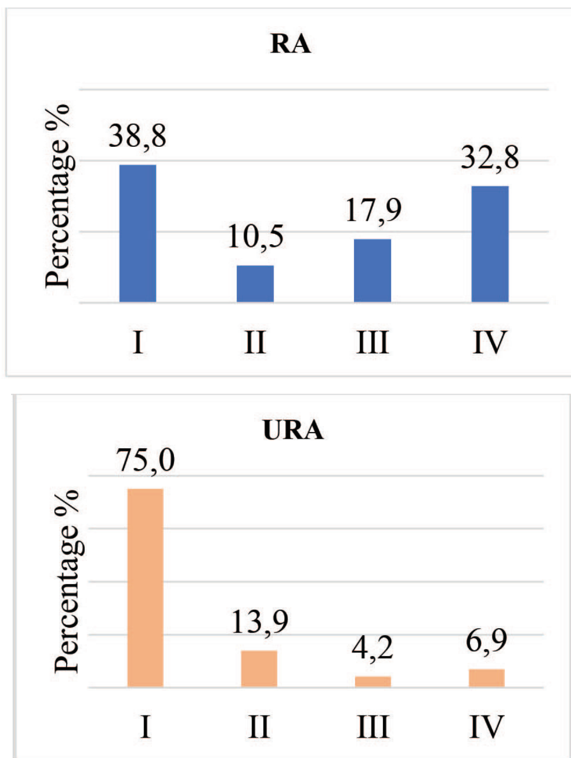

Chart 4. *Stream classification to the RA and URA*

Comments: The number of RA and URA were quite similar, with 67 and 72 aneurysms respectively. Type I still was the most common type in both RA and URA but there was a decrease in type I and moved to type III and IV in RA, respectively 4.2 % and 6.9% in URA to 17.9% and 32.8% in RA.

3.6. Size of the flow impingement region in RA and URA group

Table 6. *Size of the flow impingement region in RA and URA group*

Size of the flow impingement region	RA	URA	Total	p
Large	25 (30,1)	58 (69,9)	83 (100)	<0,01
Small	42 (75,0)	14 (25,0)	56 (100)	
Total	67 (48,2)	72 (51,8)	139 (100)	

Comments: RA with a small size of flow impingement region accounted for 42/67 RA (62.7%). In the small size, there were 42/56 RA (75%). In URA, the large size percentage was higher than the small size, 80.5%, and 19.5% respectively. There was a significant statistical difference between the number of URA and RA in the large size of the flow impingement region, p < 0.01.

3.7. Size of the inflow jet in RA and URA group

Table 7. *Size of the inflow jet in RA and URA group*

Size of the inflow jet	RA	URA	Total	p
Large	23 (29,1)	56 (70,9)	79 (100)	<0,01
Small	44 (73,3)	16 (26,7)	60 (100)	
Total	67 (48,2)	72 (51,8)	139 (100)	

Comments: In the small size of IJ, the number of RA was higher than the URA, 73.3% and 26.7% respectively. While the small size was more common than the large size in RA (65.7% and 34.3% respectively), it was inversed in URA, 77.8% for large size, and 22.2% for small size. There was a significant statistical difference between the number of URA and RA in the large size of the IJ, p < 0.01.

IV. DISCUSSION

1. Demographic characteristics

In our study, 127 patients with a range age from 27 to 84 years old, the average age was 56.31± 12.54. The most common age group was from 50 to 70 years old, 72/127 patients (56.7%) which is similar to previous studies, 54 years old in Killer et al[7] and 52.9 years old in Vu et al [8].

Females dominated the study, 80 females (63%) versus 47 males (37%). The rate of women is 1.7 times that of men and similar to studies of Cebral and Vu (2.0 and 1.2, respectively). Their gender ratio is quite consistent with other studies in Vietnam. The reason why women have more brain aneurysms than men is thought to be due to the thinner vessel wall structure, as well as the influence of the hormone estrogen.

This study included 127 patients with a cerebral aneurysm, of which 66 patients (52%) had RA and 61 patients (48%) had URA. Previously, in Vietnam, most of the patients were admitted to the hospital with a ruptured aneurysm, only then discovered aneurysms were treated, so there were almost no reports on the treatment of unruptured aneurysms. With the development of noninvasive diagnostic modalities such as MSCT and MRI, it is possible to detect more unruptured TPs. Number of 48% unruptured TP was treated, demonstrating the effectiveness of non-invasive diagnostic methods.

2. CA characteristics

Aneurysms were distributed mainly in the carotid system with 88 aneurysms (51.8%), followed by aneurysms of anterior communicating arteries (18.2%), and posterior communicating arteries (10. ,6%). The least common are aneurysms in the posterior cerebral circulation.

Small aneurysms (<5mm) accounted for the majority (66.5%) in this study and only 7.1% are large aneurysms. The mean diameter of the aneurysm was 4.83±2.73. The result is consistent with most of the authors when admitting that aneurysms have a small size that makes up the majority.

3. Aneurysm flow characteristics

The largest flow appeared at the neck and the inlet flow was 3.15 ml/s and 3.14 ml/s, respectively. The lowest flow at the dome when the mixed turbulent blood flow is 2.28 ml/s. These are average numbers over the entire duration of 1 cardiac cycle and do not completely reflect the actual flow at each time. For example, at the dome of the aneurysm, the minimum flow is 0.6ml/s and the maximum is 7.8ml/s, and the average flow at the neck is 3.15ml/s, the smallest is 0.8ml/s, the maximum is 8.9ml/s. This means that there are times when the flow velocity at the dome is higher at the neck but smaller on average over the whole time, indicating that the variation in internal flow is highly dependent on the variation of the eddy current, parent flow, and the factors of the aneurysm as the expansion of the aneurysm to accommodate the variation in internal flow. This is seen when we compare the ruptured and unruptured aneurysms, especially the position of the aneurysm dome.

4. Hemodynamic characteristics of the aneurysm

In our study, the inflow was most frequent in the distal part of the neck, impacting the wall at the basal position (64.8%), or the trunk (29.1%). Only 15% of aneurysms have flow impinging on the neck of the aneurysm. Compared with the study of JR Cebral et al., the inflow was common at the base (47%), trunk (27%), and 20% of aneurysms with flow affecting the neck of the aneurysm [9].

According to Cebral's classification based on inflow and eddy formation as well as eddy stability, flow type I (57.6%) is the most common, followed by type IV (19 .4%), type II (12.2%) and type III (10.8%) compared with the study by JR Cebral are quite similar with flow type I (44%) being the most common, followed by type IV (20%), type II (19%), and class III (17%) [9].

The number of ruptured and unruptured aneurysms is quite similar. The majority has still flowed phenotype I in both ruptured and unruptured aneurysms, but there is a great reduction in flow phenotype number I, which gradually shifts to flow pattern III and IV in the ruptured group, respectively. from 4.2% and 6.9% of the unruptured group to 17.9% and 32.8% compared with the study of JR Cebral in flow type I and II, unruptured aneurysms accounted for 73 % and 55% of aneurysms in these groups. In types III and IV, the number of ruptured aneurysms exceeded the number of unruptured aneurysms, reaching 60% and 58% of the total, respectively. There is a similarity between the two studies where flow patterns I, II are common in unruptured aneurysms and III, IV are seen more frequently in ruptured aneurysms, indicating that the inflow status changes and changes stabilization of vortices inside aneurysms as well as the establishment and destruction of vortices in ruptured aneurysms.

The flow impingement region factor: The number of RA and URA are quite similar. The RA group had a high percentage of small size, 42/67 (62.7%). In the small size group of the impingement region, 42 RA out of 56 aneurysms (75%). Conversely, the group of unruptured aneurysms had a high rate of large size, 58/72 (80.5%). there was a statistically significant difference between RA and URA in the large-size group.

Inflow jet size factor: RA with a small size of inflow jet has a high proportion, 44/67 (65.7%) much more than unruptured aneurysms. In the small size, the rate of RA was up to 73.3%. In contrast, large inflow jet sizes account for a high proportion in URA, 56/ 72 (77.8%). In large inflow jet size, there was a statistically significant difference between RA and URA, $p<0.01$.

Compared with the study of JR Cebral, it is quite similar with the relative size of the impingement region with a dominant difference, more than 80% of ruptured aneurysms have a small impingement region, accounting for 65% total small size of the impingement region. In contrast, URA accounts for 82% of aneurysms with a large size of impingement relative to the size of the aneurysm dome. Most ruptured aneurysms were found to be of small size (76%), accounting for 54% of aneurysms in this category. In contrast, 75% of large-size aneurysms do not rupture.

Thus, the simple stable vortex patterns, a large area of influence, and large beam size are often seen with unruptured aneurysms. In contrast, ruptured aneurysms are more likely to have disturbed flow patterns, small areas of influence, and narrow inflow.

V. CONCLUSION AND RECOMMEND

The inflow is mainly at the distal neck location, affecting mainly the base of the aneurysm. The flow at the inlet site is the largest, the lowest at the base of the aneurysm. Based on the JR Cebral's grading of a simple stable vortex model, the large impingement region and large inflow jet size are commonly seen with unruptured aneurysms. In contrast, ruptured aneurysms have a disturbed eddy flow pattern, a small impingement, and a narrow inlet flow.

Measurement of flow inside an aneurysm using the optical flow principle combined with fluid dynamics simulation using numerical analysis is a new method to better understand hemodynamics inside aneurysms. Factors such as JR Cebral flow grade, impingement zone, impingement zone size, and inflow jet size should be taken into consideration as a factor to consider for the rupture risk of a UR for a follow-up plan with appropriate monitoring and treatment.

A1

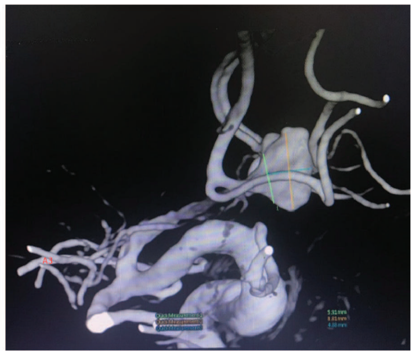

A2

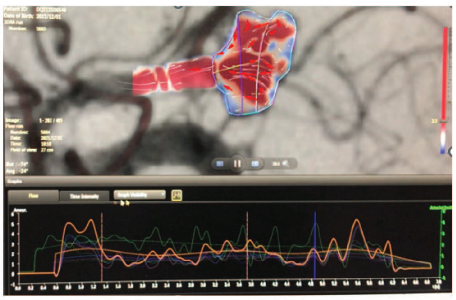

B

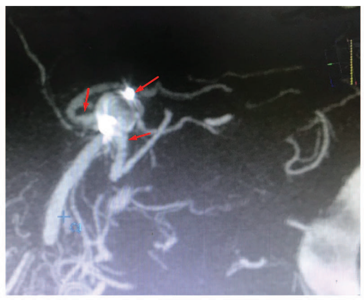

C

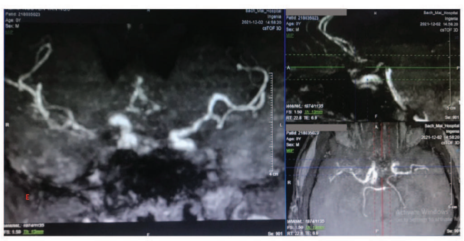

D

Figure 2. *A case with anterior communication artery aneurysm*

Patient Nguyen Van N, male, 63 years old (archive code I66/196) was admitted to the hospital because of a coma with a Glassgow score of 9 points. CT scan showed images of subarachnoid hemorrhage due to rupture of anterior communicating artery aneurysm. Then, the patient was taken DSA (figure A1-A2) in which there was a large aneurysm with a wide neck, right-angled neck, irregular margins with many sharp knobs, two A2 branches separating from the neck of an aneurysm, swirling inflow pattern into different currents, which impact on many places in the aneurysm, forming and destroying vortices, can be classified as type IV flow (figure B) and flow inside the aneurysm (figure B). The patient had a hospital consultation with an indication for emergency WEB placement (figure C). Taken again after 1 day, the A2 branches showed well without cerebral infarction (Figure D). The patient then gradually stabilized and was discharged after 10 days.

REFERENCE

1. Osborn AG. *Diagnostic Cerebral Angiography*. Lippincott Williams & Wilkins; 1999.
2. Vega C, Kwoon JV, Lavine SD. Intracranial Aneurysms: Current Evidence and Clinical Practice. *AFP*. 2002;66(4):601.
3. Johnston SC, Higashida RT, Barrow DL, et al. Recommendations for the endovascular treatment of intracranial aneurysms: a statement for healthcare professionals from the Committee on Cerebrovascular Imaging of the American Heart Association Council on Cardiovascular Radiology. *Stroke*. 2002;33(10):2536-2544. doi:10.1161/01.str.0000034708.66191.7d
4. Bonnefous O, Pereira VM, Ouared R, et al. Quantification of arterial flow using digital subtraction angiography. *Med Phys*. 2012;39(10):6264-6275. doi:10.1118/1.4754299
5. Pereira VM, Ouared R, Brina O, et al. Quantification of internal carotid artery flow with digital subtraction angiography: validation of an optical flow approach with Doppler ultrasound. *AJNR Am J Neuroradiol*. 2014;35(1):156-163. doi:10.3174/ajnr.A3662
6. Brina O, Ouared R, Bonnefous O, et al. Intra-Aneurysmal Flow Patterns: Illustrative Comparison among Digital Subtraction Angiography, Optical Flow, and Computational Fluid Dynamics. *AJNR Am J Neuroradiol*. 2014;35(12):2348-2353. doi:10.3174/ajnr.A4063
7. Killer-Oberpfalzer M, Kocer N, Griessenauer CJ, et al. European Multicenter Study for the Evaluation of a Dual-Layer Flow-Diverting Stent for Treatment of Wide-Neck Intracranial Aneurysms: The European Flow-Redirection Intraluminal Device Study. *AJNR Am J Neuroradiol*. 2018;39(5):841-847. doi:10.3174/ajnr.A5592
8. Vu Dang Luu. Clinical features and imaging characteristics of computed tomography and DSA of ruptured cerebral aneurysm. Evaluation of the effectiveness of embolization for treatment of the ruptured cerebral aneurysm. Thesis Doctor of Medicine, Hanoi Medical University. 2012.
9. Cebral JR, Castro MA, Burgess JE, Pergolizzi RS, Sheridan MJ, Putman CM. Characterization of cerebral aneurysms for assessing risk of rupture by using patient-specific computational hemodynamics models. *AJNR Am J Neuroradiol*. 2005;26(10):2550-2559.

Correspondent: Nguyen Van Hoang. Email: hoangnguyen96.hmu@gmail.com
Recieved: 21/10/2022. Assessed: 22/10/2022. Reviewed: 09/12/2022. Accepted: 21/12/2022